Citation: Cell Death and Disease (2011) 2, e156; doi:10.1038/cddis.2011.39

www.nature.com/cddis

# Blockade of Hsp90 by 17AAG antagonizes MDMX and synergizes with Nutlin to induce p53-mediated apoptosis in solid tumors

AV Vaseva[1,2,3], AR Yallowitz[2,3], ND Marchenko[2], S Xu[2] and UM Moll[2]

**Strategies to induce p53 activation in wtp53-retaining tumors carry high potential in cancer therapy. Nutlin, a potent highly selective MDM2 inhibitor, induces non-genotoxic p53 activation. Although Nutlin shows promise in promoting cell death in hematopoietic malignancies, a major roadblock is that most solid cancers do not undergo apoptosis but merely reversible growth arrest. p53 inhibition by unopposed MDMX is one major cause for apoptosis resistance to Nutlin. The Hsp90 chaperone is ubiquitously activated in cancer cells and supports oncogenic survival pathways, many of which antagonize p53. The Hsp90 inhibitor 17-allylamino-17-demethoxygeldanamycin (17AAG) is known to induce p53-dependent apoptosis. We show here that in multiple difficult-to-kill solid tumor cells 17AAG modulates several critical components that synergize with Nutlin-activated p53 signaling to convert Nutlin's transient cytostatic response into a cytotoxic killing response *in vitro* and in xenografts. Combined with Nutlin, 17AAG destabilizes MDMX, reduces MDM2, induces PUMA and inhibits oncogenic survival pathways, such as PI3K/AKT, which counteract p53 signaling at multiple levels. Mechanistically, 17AAG interferes with the repressive MDMX–p53 axis by inducing robust MDMX degradation, thereby markedly increasing p53 transcription compared with Nutlin alone. To our knowledge Nutlin + 17AAG represents the first effective pharmacologic knockdown of MDMX. Our study identifies 17AAG as a promising synthetic lethal partner for a more efficient Nutlin-based therapy.**

*Cell Death and Disease* (2011) **2,** e156; doi:10.1038/cddis.2011.39; published online 12 May 2011
**Subject Category:** Cancer

Fifty percent of human tumors retain wild-type (wt) p53, albeit with inadequate function due to abnormalities in p53 regulation or defective p53 pathway signaling. Mechanisms that suppress wtp53 function in tumors include overexpression of the p53 repressors murine double minute-2 (MDM2) and murine double minute-X (MDMX).[1] The concept of targeted reactivation of wtp53 for therapy is greatly strengthened by mouse models, where genetic restoration of p53 in established tumors leads to clinical tumor regression.[2,3] Thus, pharmacological strategies to induce p53 activation in human tumors carry high potential in cancer therapy. Nutlin-3a is a potent and highly selective small-imidazoline-based MDM2 inhibitor. It blocks MDM2-mediated p53 degradation and transcriptional repression, thereby leading to non-genotoxic p53 stabilization and activation of growth arrest and apoptosis.[4–6]

Nutlin promotes cell death in cultured leukemia cells, select osteosarcoma cells and their xenografts.[7,8] It is currently undergoing phase-I and II clinical trials for hematologic and some solid malignancies in combination with conventional chemotherapeutics.[6,7] However, its clinical development has been plagued by a major roadblock that became apparent for most solid cancers. Although Nutlin efficiently induces transient cell-cycle arrest, pre-clinical and clinical data from a wide array of solid tumors indicate that it is inefficient in inducing definitive apoptosis.[9–11] Thus, turning Nutlin into an efficient cytotoxic killer by identifying a synthetic lethal partner drug is of paramount clinical importance.

Mechanistically, robust upregulation of Nutlin-induced p21, concomitant with attenuated expression of pro-apoptotic genes, has long been thought to be a major reason why many tumors merely undergo reversible growth arrest rather than apoptosis upon exposure to Nutlin.[9–11] However, while the p21 link is true after genotoxic p53 activation, one recent *in vitro* study found that high p21 levels after non-genotoxic Nutlin-induced p53 activation did not protect solid cancer cells from apoptosis, which puts this mechanism into question for some circumstances.[12] Alternatively, and not mutually exclusive, p53 inhibition by the remaining MDMX was proposed as a cause for apoptosis resistance after exposure to Nutlin.[13] Although MDMX is highly homologous to MDM2, Nutlin is inefficient in interrupting the transcription-repressive MDMX–p53 complex, which prevents p53 transcriptional activity in numerous cancer cell lines, including retinoblastomas, which harbor MDMX upregulation.[13–16] Indeed, knockdown of MDMX by RNAi renders Nutlin more efficient in promoting the apoptosis of cultured tumor cells.[15,17]

[1]Graduate program in Molecular and Cellular Biology, Stony Brook University, Stony Brook, NY 11794, USA and [2]Department of Pathology, Stony Brook University, Stony Brook, NY 11794, USA
Corresponding author: UM Moll, Department of Pathology, Stony Brook University, Nichols Road, Stony Brook, NY 11794-8691, USA. Tel: 631 444 2459; Fax: 631 444 3424; E-mail: umoll@notes.cc.sunysb.edu
[3]These authors contributed equally to the work.
**Keywords:** Nutlin; 17AAG; wtp53; synergy; cytotoxicity
**Abbreviations:** wtp53, wild-type p53; MDM2, murine double minute-2; MDMX, murine double minute-X; Hsp90, heat-shock protein-90; 17AAG, 17-allylamino-17-demethoxygeldanamycin; 17DMAG, 17-dimethylaminoethylamino-17-demethoxy-geldanamycin; PUMA, p53 upregulated modulator of apoptosis; PARP, poly(ADP-ribose)polymerase; PI3K, phosphatidylinositol-3-kinase; AKT, serine/threonine protein kinase-B; PI, propidium iodide
Received 10.3.11; accepted 10.3.11; Edited by G Melino

Here we show that the apoptotic efficiency of Nutlin for solid tumor cells *in vitro* and in xenografts is dramatically enhanced when combined with the non-genotoxic heat-shock protein-90 (Hsp90) inhibitor 17-allylamino-17-demethoxygeldanamycin (17AAG). The Hsp90 chaperone complex is highly upregulated and cancer cells are addicted to Hsp90 for their survival. Mechanistically, 17AAG interferes with the repressive MDMX–p53 complex and induces robust MDMX degradation, thereby increasing p53 transcriptional activity by about 2.5-fold compared with Nutlin alone. In addition, 17AAG affects other anti-p53 regulatory pathways such as the phosphatidylinositol-3-kinase (PI3K)/serine/threonine protein kinase-B (AKT) pathway that depend on Hsp90. As Nutlin and Hsp90 inhibitors are currently undergoing separate clinical trials, our results provide a molecular rationale for a more efficient Nutlin-based anticancer therapy by concomitantly targeting an essential anti-p53 directed cofactor.

## Results

**17AAG enhances wtp53 signaling by stabilizing p53, destabilizing MDMX and disrupting p53–MDMX interaction.** The Hsp90 chaperone machinery is highly and almost ubiquitously activated specifically in cancer cells[18] and p53 is an important client protein. The aberrant conformation of mutant p53 proteins requires permanent heat-shock support; thus mutant p53 is stably engaged in Hsp90 complexes to prevent aggregation.[19,20] For wtp53, Hsp90 also fulfills an important role by promoting its proper conformation through transient interaction.[21–23] Importantly, inhibition of Hsp90 by the highly specific geldanamycin-derived Hsp90 inhibitor 17AAG or 17-dimethylaminoethylamino-17-demethoxy-geldanamycin (17DMAG) was reported to increase wtp53 protein in cancer cells[24,25] and induce apoptosis in a wtp53-dependent manner in both mouse embryo fibroblasts and in allotransplanted primary medulloblastomas *in vivo*.[25]

We therefore first examined how 17AAG affects wtp53 and its negative regulators MDMX and MDM2. A panel of randomly selected wtp53 human cancer cell lines from solid tumors (RKO colorectal, MCF7 breast, AGS gastric adenocarcinoma and U2OS osteosarcoma) were treated with 17AAG to assess protein levels. As expected, in all four cell lines 17AAG increased p53 significantly within 4–8 h (Figure 1a). Surprisingly, 17AAG dramatically decreased the level of MDMX protein in all the lines tested. Concomitant downregulation of MDM2 was observed in RKO and AGS, whereas p21 protein was upregulated in all the lines (Figure 1a).

To determine the extent to which these changes in protein expression were due to transcriptional regulation, we performed qRT-PCR on 17AAG-treated cells. 17AAG increased both p53 mRNA and protein stability (Figure 1b). Consequently, 17AAG increased the gene expression of the classic p53 targets MDM2, p21 and p53 upregulated modulator of apoptosis (PUMA), validating p53 activation (Figure 1c). However, concerning MDM2 protein, 17AAG promoted MDM2 destabilization (see Figure 1a), consistent with MDM2 also being an Hsp90 client.[20] Of note, MDMX message levels remained unaffected by 17AAG in this system, indicating that downregulation of MDMX protein occurred mainly at the posttranscriptional level (Figure 1c). The pan-caspase inhibitor Z-VAD did not block MDMX destabilization (whereas the proteasome inhibitor ALLN did), indicating that 17AAG-induced MDMX destruction was a primary cellular response, rather than simply a secondary caspase-mediated degradation event. By contrast, the latter was the case for the observed MDM2 degradation in RKO cells (Figure 1d). As ALLN stabilized both MDMX and MDM2 upon 17AAG exposure, this also indicated that 17AAG did not interfere with proteasome degradation (Figure 1d, right).

As Hsp90 binds to MDM2 and p53,[20,21] and MDM2 binds to p53 and MDMX,[26] we determined whether 17AAG could affect these interactions. Importantly, in co-immunoprecipitations 17AAG rapidly disrupted the complex between MDMX and p53 within 2 h of treatment, a time point when MDMX levels were still not affected (Figure 1e, left). Furthermore, 17AAG disrupted the MDMX–MDM2 complex (Figure 1e, left) possibly explaining the rapid p53 accumulation. Additionally, 17AAG also disrupted the Hsp90–MDM2 complex (Figure 1e, right), but did not affect the MDM2–p53 interaction (Figure 1e, left).

**17AAG kills cancer cells in a wtp53-dependent manner.** In MEFs and allotransplanted primary murine medulloblastomas, 17AAG was shown to induce apoptosis in a wtp53-dependent manner.[25] To examine whether this also holds true for human cancer cells, we compared the response of the isogenic colorectal cancer pair HCT116 p53+/+ and p53−/− to17AAG. As already seen for other wtp53 lines, 17AAG treatment of HCT116 p53+/+ increased their p53, p21 and PUMA protein levels but decreased their MDMX levels (Figure 2a). By contrast, HCT116 p53−/− cells lacked this response. Moreover, 17AAG-induced poly(ADP-ribose)polymerase (PARP) cleavage was largely dependent on the presence of p53 (Figure 2a).

Higher caspase activation in HCT116 p53+/+ *versus* p53−/− cells confirmed the p53 dependence of 17AAG-induced apoptosis (Figure 2b, left). This was further confirmed by significantly lower survival of p53+/+ *versus* p53−/− cells in Annexin-V/propidium iodide (PI) FACS analysis (Figure 2b, right). As expected, 17AAG also induced the transcriptional activation of p53, indicated by induction of p21, PUMA and MDM2 in p53+/+ cells only (Figure 2c). MDMX message was not affected by 17AAG in p53+/+ or p53−/− cells.

**17AAG synergizes with Nutlin to induce apoptosis in a p53-dependent manner.** As 17AAG caused p53-dependent cell death by stabilizing and activating wtp53, we reasoned that 17AAG might synergize with Nutlin to enhance net p53 signaling and induce a stronger apoptotic response than Nutlin alone. Of note, 17AAG did not disrupt the interaction between MDM2 and p53 (Figure 1e), indicating that it stabilized p53 through a mechanism different than Nutlin. We therefore treated cancer cells with Nutlin alone, 17AAG alone or a combination of Nutlin and 17AAG. Indeed, in all five lines tested, PARP cleavage was dramatically

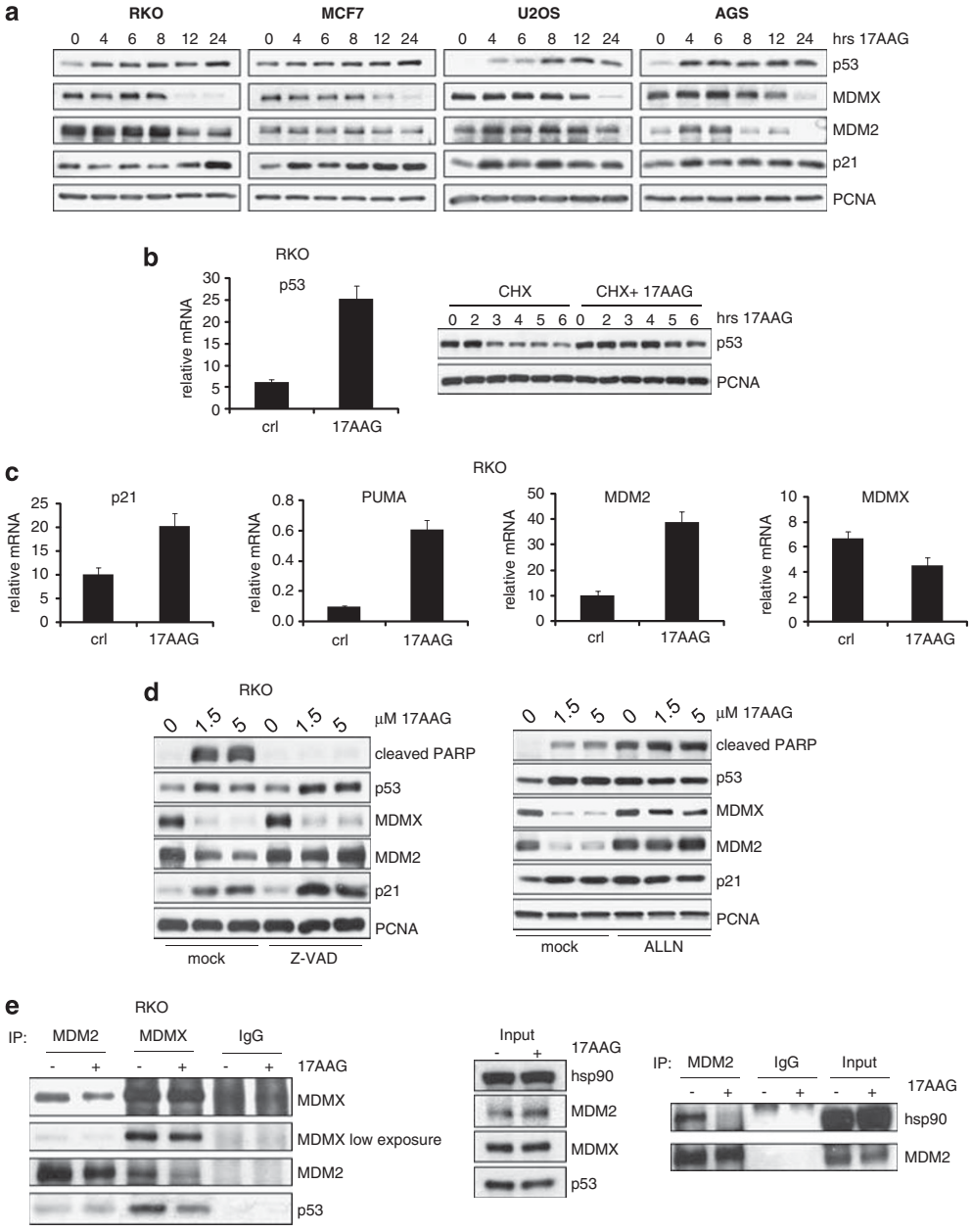


**Figure 1** 17AAG stabilizes wtp53, destabilizes MDMX and disrupts p53–MDMX interaction. (**a**) 17AAG increases p53 and p21, but decreases MDMX protein levels. RKO, MCF7, U2OS and AGS human cancer cells were treated with 2 $\mu$M of 17AAG for the indicated time periods. The levels of p53, MDMX, MDM2 and p21 proteins were analyzed by immunoblots. PCNA is a loading control. (**b**) 17AAG increases both the mRNA levels and the protein stability of p53. Left: p53 mRNA levels in RKO cells treated with 1.5 $\mu$M of 17AAG or DMSO for 24 h. qRT-PCR, mRNA levels were normalized to actin. The error bars represent standard errors from two independent experiments, each performed in triplicate. Right: Cycloheximide (CHX) chase of RKO cells treated as indicated. PCNA is a loading control. (**c**) 17AAG increases the transcription of the p53 target genes p21, PUMA and MDM2. RKO cells were treated with 1.5 $\mu$M of 17AAG or DMSO for 24 h. The mRNA levels of MDMX, p21, PUMA and MDM2 were evaluated by qRT-PCR as shown in panel **b**. (**d**) Destabilization of MDMX by 17AAG is caspase-independent and proteasome-dependent, whereas destabilization of MDM2 is a secondary caspase-dependent event. RKO cells were pretreated with 20 $\mu$M of the pan-caspase inhibitor Z-VAD-FMK (left) or 5 $\mu$M of the proteasome inhibitor ALLN (right) 1 h before adding 17AAG at the indicated doses of for an additional 24 h. (**e**) 17AAG disrupts p53–MDMX and MDM2–Hsp90 interactions. RKO cells were treated with 1.5 $\mu$M of 17AAG for 2 h followed by immunoprecipitation using MDMX or MDM2 antibodies. MDMX–p53, MDM2–MDMX and MDM2–p53 complexes (left), as well as MDM2–Hsp90 complexes (right), were detected by immunoblots. Isotype-matched IgGs serve as controls. Middle: Immunoblot indicating the relative input of the proteins used in the left panel

higher when both drugs were combined compared with each drug alone (Figures 3a and e). Similarly, caspase activation (Figure 3b and Supplementary Figure 1) and the number of Annexin-V/PI-positive apoptotic cells (Figure 3c and Supplementary Figure 2) were much higher when both drugs where combined compared with each drug alone in all seven cell lines tested (RKO, U2OS, MCF7, AGS, HCT116 p53+/+, SJSA and RPMI-1788).

To determine whether the increase in cell death after drug combination was truly synergistic rather than merely additive,

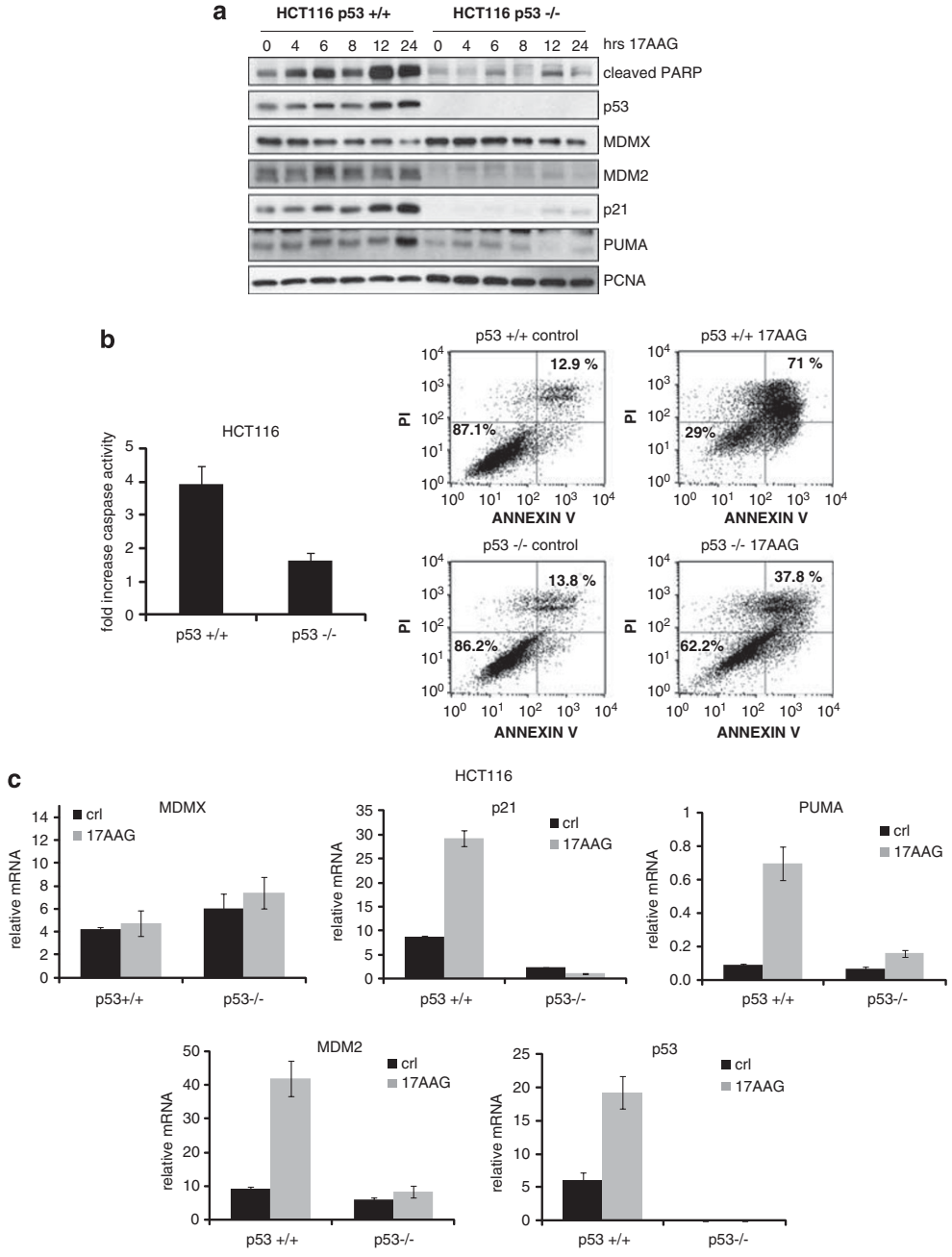


**Figure 2** 17AAG kills cancer cells in a p53-dependent manner. (**a**) In response to 17AAG, p53−/− tumor cells show much lower PARP cleavage and lack p21 and PUMA induction compared to isogenic p53 + / + cells. HCT116 p53 + / + and p53−/− cells were treated with 1.5 $\mu$M 17AAG or DMSO. The levels of the indicated proteins were analyzed by immunoblotting. (**b**) p53−/− cells are less sensitive to 17AAG-induced cell death than p53 + / + cells. Left, HCT116 p53 + / + and p53−/− cells were treated with 2 $\mu$M of 17AAG for 48 h and caspase activity was measured. The error bars represent standard errors from four replicates. Right, HCT116 p53 + / + and p53−/− cells were treated with 2 $\mu$M of 17AAG for 72 h, processed for Annexin-V and PI staining and measured by FACS. % survival (Annexin-V/PI double-negative population) is indicated in the lower left quadrant and total % death is indicated in the upper right quadrant. (**c**) 17AAG induces the transcription of p53 target genes p21, PUMA and MDM2 in p53 + / + but not in p53−/− cells. HCT116 p53 + / + and p53−/− cells were treated with 1.5 $\mu$M of 17AAG or DMSO for 24 h. mRNA levels were measured by qRT-PCR and normalized to actin. The error bars represent standard errors from two independent experiments, each performed in triplicate

we calculated combinatorial indexes (CIs). A CI value $<1$ indicates synergism; CI $=1$ indicates additive effects and CI $>1$ indicates antagonism.[27] In all four lines tested, the CI was $<1$ ranging from 0.23 to 0.33, confirming strong synergistic effects of the 17AAG/Nutlin combination in all the cases (Figure 3d). The 17AAG/Nutlin combination induced significant PARP cleavage and caspase activation in HCT116 p53 + / + cells but not in p53−/− cells, verifying that this synergistic effect was p53-dependent (Figure 3e).

**17AAG destabilizes MDMX protein in Nutlin-treated cancer cells and can potentiate Nutlin-induced p53 transcription of PUMA.** Next, we examined how 17AAG might modulate Nutlin-induced p53 signaling to explain its

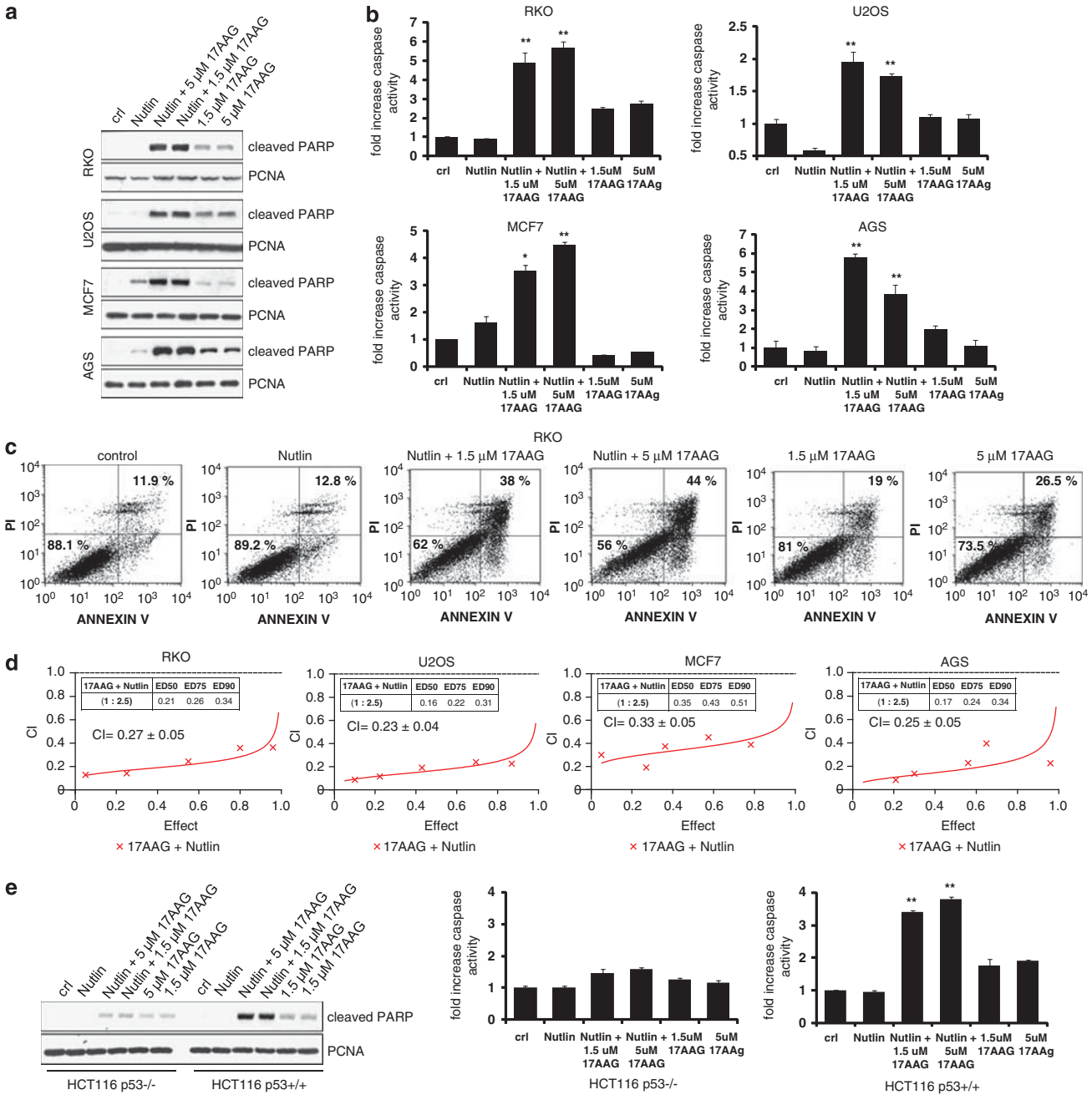


**Figure 3** 17AAG synergizes with Nutlin to induce apoptosis in a p53-dependent manner. (**a**) Combined treatment of 17AAG and Nutlin significantly increases PARP cleavage compared with each single treatment. RKO, U2OS, MCF7 and AGS cells were pretreated with 1.5 or 5 $\mu$M of 17AAG for 1 h, followed by 10 $\mu$M of Nutlin for an additional 24 h where indicated. Treatment with 17AAG alone was for 24 h. Controls received no treatment. PARP cleavage was analyzed by immunoblotting using an antibody that only recognizes cleaved PARP. PCNA is a loading control. (**b**) Increase of caspase activity upon combined treatment. The indicated cell lines were treated as shown in panel **a** and caspase activity was measured. The error bars represent standard errors from four replicates. * denotes $P<0.05$; ** denotes $P<0.005$ comparing Nutlin to Nutlin + 17AAG. (**c**) Increase of cell death upon combined treatment. RKO cells were treated as above and measured by FACS for Annexin-V and PI staining. % survival (Annexin-V/PI double-negative population) is indicated in the lower left quadrant and total % death is indicated in the upper right quadrant. (**d**) Synergistic induction of cell death by Nutlin + 17AAG. The indicated cell lines were treated with increasing doses of 17AAG or Nutlin alone or with combinations at a fixed ratio for 72 h. The % of dead cells was determined by trypan blue exclusion assays. CIs were calculated by the isobologram analysis using the CalcuSyn software.[27] (**e**) The combination of Nutlin + 17AAG increases cell death in p53 + / + but not in p53−/− cells. HCT116 p53 + / + or p53−/− cells were treated as shown in panel **a**. PARP cleavage (left) and caspase activity (right) were analyzed. The error bars represent standard errors from four replicates. **denotes $P<0.005$ comparing Nutlin to Nutlin + 17AAG

synergism in promoting Nutlin-induced apoptosis. In engineered H1299 cell systems with ectopic wtp53, it was previously shown that p53 levels can be a determinant of arrest (lower levels) *versus* apoptosis (higher levels).[28] However, in our cell lines, endogenous p53 did not further increase with Nutlin + 17AAG compared with Nutlin alone (Figure 4a). Thus, increased apoptosis was not simply due to higher p53 levels.

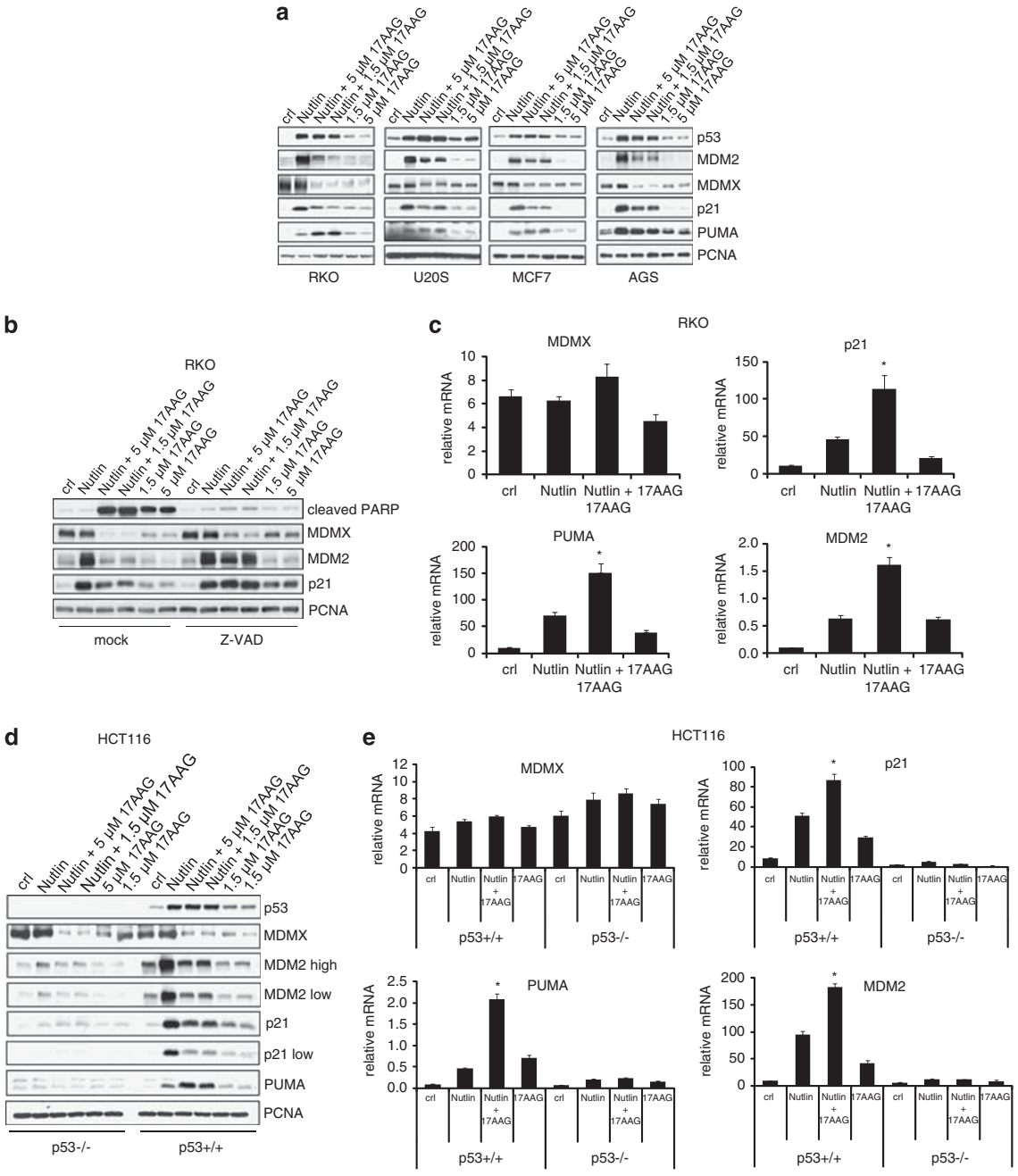


**Figure 4** 17AAG destabilizes MDMX in Nutlin-treated cancer cells and potentiates Nutlin-induced p53 transcription of PUMA in some cancers. (**a**) 17AAG decreases MDMX, can increase PUMA and decreases MDM2 and p21 levels in Nutlin-treated cells. Cells were pretreated with 1.5 or 5 $\mu$M of 17AAG for 1 h, followed by 10 $\mu$M of Nutlin for an additional 24 h where indicated. Treatment with 17AAG alone was for 24 h. PCNA is a loading control. (**b**) 17AAG-induced downregulation of MDMX upon Nutlin treatment is not a secondary caspase-dependent event. RKO cells were pretreated with 20 $\mu$M of the pan-caspase inhibitor Z-VAD-FMK or mock diluent-treated for 1 h prior to adding Nutlin (10 $\mu$M) and/or 17AAG alone as indicated. (**c**) 17AAG potentiates Nutlin-induced transcription of p21, PUMA and MDM2. RKO cells were treated as shown in panel **a** and the mRNA levels of the indicated genes were assessed by qRT-PCR, normalized to actin levels. The error bars represent standard errors from two independent experiments, each performed in triplicate. *denotes $P<0.05$ comparing Nutlin to Nutlin + 17AAG. (**d**) The effect of 17AAG on Nutlin-induced PUMA, MDM2 and p21 proteins is p53-dependent. HCT116 p53 + / + and p53 − / − cells were treated and analyzed as shown in panel **a**. (**e**) The effect of 17AAG on the Nutlin-induced transcription of PUMA, MDM2 and p21 is p53-dependent. HCT116 p53 + / + and p53 − / − cells were treated as shown in panel **a** and mRNA levels were determined by qRT-PCR. The data are normalized to actin. The error bars represent standard errors from two independent experiments, each performed in triplicate. *denotes $P<0.05$ comparing Nutlin to Nutlin + 17AAG

Importantly, in the presence of Nutlin, 17AAG still decreased MDMX protein levels, and in most cases sharply (RKO, AGS and HCT116) (Figure 4a). Again, this combined drug-mediated MDMX destruction was primarily a caspase-independent effect, as shown by Z-VAD treatment (Figure 4b). The robust MDMX degradation coincided with a

further surge of the p53 transcriptional response compared with Nutlin or 17AAG alone, as judged by the representative induction of p21, PUMA and MDM2 targets (Figure 4c).

On the protein level, addition of 17AAG induced differential regulation of these three Nutlin-induced p53 targets, likely due to direct or indirect Hsp90 influence on their stability, which altogether likely generated the apoptosis-promoting drug effects. Importantly, PUMA protein was significantly upregulated in RKO, MCF7 and HCT116 cells upon combined treatment compared with Nutlin or 17AAG alone (Figures 4a and e). Nutlin alone invariably induced the robust upregulation of the p53 target MDM2 (Figure 4a).[6] At the same time, non-toxic doses of Nutlin – although to a very significant extent – do not completely disrupt all p53–MDM2 complexes, creating a dampening loop that decreases its maximum efficiency.[29] Interestingly, Nutlin + 17AAG significantly downregulated MDM2 protein levels compared with Nutlin alone in all five lines tested (Figures 4a and d). This was a secondary caspase-mediated effect as it was blocked by Z-VAD (Figure 4b). Thus, although not affecting p53 levels, by lowering inhibitory MDM2, the 17AAG co-drug possibly also enhanced Nutlin's efficacy by relieving MDM2's repression on p53 as well (Figure 4c). Nutlin invariably induces the robust induction of p21 protein,[9–11] again seen here (Figures 4a and d). However, the Nutlin-induced p21 induction was significantly suppressed toward near-basal levels by concomitant 17AAG exposure (Figures 4a and d). While robust p21 induction has been considered a major determinant of the Nutlin-associated apoptosis resistance,[9–11] one study of seven cancer lines (three of which overlapped with ours) found p21 irrelevant in protecting Nutlin-treated cells from apoptosis.[12] Thus, the combination-induced p21 downregulation that we observed might not contribute to enhanced apoptosis, at least in some cancers.

Finally, the modulating effect of 17AAG on the protein stability (Figure 4d) and transcription (Figure 4e) of Nutlin-induced p21, PUMA and MDM2 was p53-dependent, as it was only present in HCT116 p53 + / + but not in p53 − / − cells. As well, degradation of MDMX incurred by 17AAG was not p53-dependent (Figure 4d).

**Nutlin synergizes with 17AAG in part by inhibiting MDMX and AKT signaling.** Although MDMX is highly homologous to MDM2, Nutlin is inefficient at interrupting the repressive MDMX–p53 complex. Nutlin binds to MDM2 *versus* MDMX with a 40-fold stronger inhibition constant ($K_i$ of 0.7 *versus* 28 $\mu$M), whereas MDMX and MDM2 bind to p53 with similar affinities ($K_d = 0.5\ \mu$M).[6,30] Thus, in the presence of Nutlin, MDMX is still able to bind to p53 and repress its transcriptional activity.[13,14] Consequently, knockdown of MDMX was reported to potentiate Nutlin-induced apoptosis.[13–15] We confirmed these findings. When Mdmx was downregulated by siRNA in U2OS and RKO cells treated with Nutlin, PUMA (and p21) and apoptosis were significantly higher compared to scrambled siRNA-treated controls (Figure 5a). Likewise, the fact that 17AAG downregulated the MDMX protein in all the cancer lines tested (Figures 1a and 4a, b and e), disrupted the MDMX–p53 complex (Figure 1e) and effectively converted Nutlin-induced arrest into apoptosis, strongly suggested that the 17AAG-induced MDMX destruction is an important cause of apoptotic synergism between Nutlin and 17AAG. Indeed, in support of a causal relationship, stable overexpression of MDMX strongly suppressed apoptosis upon combined Nutlin + 17AAG treatment, as indicated by inhibition of PARP cleavage and caspase activity (Figures 5b and c). Moreover, MDMX overexpression also reduced Nutlin-induced PUMA and p21 levels (Figure 5b, compare lanes 2 and 9). Altogether, these results indicated that the 17AAG-mediated destruction of MDMX is indeed one strong determinant for promoting a Nutlin death response.

Many client proteins of Hsp90 are oncogenes that depend on permanent chaperone support. Thus, the Hsp90 inhibitor 17AAG affects multiple oncogenic signaling pathways, many of which participate in antagonizing p53 signaling.[18] Therefore, it is very likely that other events besides downregulation of MDMX could contribute to the apoptotic synergism between 17AAG and Nutlin. PI3K and its downstream effector AKT phosphorylate p53, MDM2 and MDMX, in sum negatively modulating p53 activity.[26] Importantly, 17AAG was reported to impair AKT stability and activity,[18,31] and we confirmed this in all the cell lines tested (Figure 5d). Although transient activation of AKT was observed, by 12 h phosphorylated AKT was almost completely lost in all the cell lines. Of note, inhibitors of the PI3K/AKT pathway can also potentiate Nutlin-induced cell death.[32,33] We confirmed enhanced PARP cleavage and caspase activity when Nutlin was combined with the PI3K inhibitor LY294002 (Figure 5e). Interestingly, identical to 17AAG (Figure 4a), the PI3K inhibitor markedly enhanced Nutlin-induced PUMA expression (Figure 5e, compare lanes 2 with 3 and 4). Therefore, the induction of PUMA by 17AAG might partly also be indirect through its effect on AKT. Overall this suggested that Nutlin synergizes with 17AAG in part also by inhibiting AKT signaling.

**Nutlin and 17AAG synergistically prevent tumor growth *in vivo* by inducing apoptosis.** To further support the functional synergism between Nutlin and 17AAG *in vivo*, we monitored its antitumor effects on tumor xenografts. We chose RKO cells as they were completely resistant to apoptosis mediated *in vitro* by Nutlin alone and are able to recover from Nutlin-mediated arrest.[9,10] Nude mice were injected with $5 \times 10^6$ RKO cells per flank and after 12 days when tumors had reached a volume of 200–300 $mm^3$ (called day 0), mice were randomized into four treatment groups of vehicle, Nutlin, 17AAG and Nutlin + 17AAG (Figure 6a).

At day 11, tumors of mice continuously treated with Nutlin alone or 17AAG alone had completely failed to respond and increased about five-fold in volume, identical to that in the vehicle controls. By contrast, tumors treated with combined Nutlin + 17AAG had increased only three-fold. Moreover, at day 15 tumors of mice treated with Nutlin + 17AAG had reached a plateau and remained stable thereafter, whereas tumors treated with Nutlin alone or 17AAG alone further accelerated their growth. In fact, both Nutlin mice, one vehicle mouse and one 17AAG mouse had to be killed at day 15 because they had reached the allowable limit of tumor burden (2 $cm^3$). By contrast, one Nutlin + 17AAG mouse needed to be killed not because of excessive tumor burden, but because of treatment-induced necrosis of one of its tumors. Over the

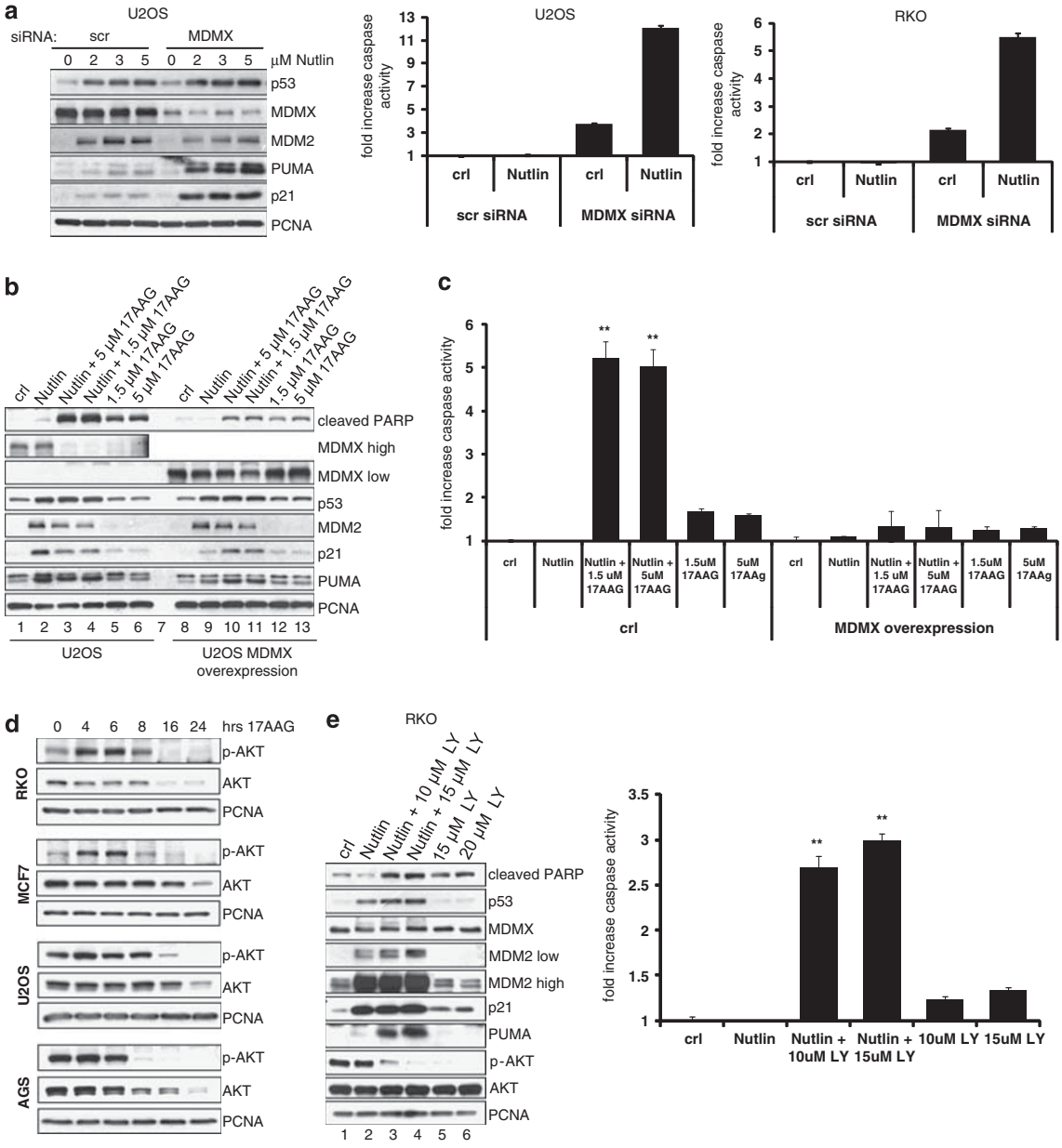


**Figure 5** 17AAG synergizes with Nutlin by inhibiting MDMX and AKT signaling. (**a**) Downregulation of MDMX enhances Nutlin-induced PUMA and apoptosis. U2OS and RKO cells were transfected with scrambled or MDMX siRNA for 24 h, followed by treatment with Nutlin (10 $\mu$M) for an additional 24 h. Left: Immunoblots, PCNA, loading control. Right: Caspase activity. (**b**) Overexpression of MDMX suppresses the Nutlin + 17AAG-induced PARP cleavage. U2OS cells stably harboring doxycycline-inducible MDMX were treated with 100 ng/ml doxycycline overnight to induce MDMX expression. Parental U2OS cells were treated with the same dose of doxycycline for the same time period. 17AAG and/or 10 $\mu$M Nutlin were added for an additional 24 h where indicated. PCNA is a loading control. (**c**) Overexpression of MDMX suppresses the Nutlin + 17AAG-induced apoptosis. U2OS parental and MDMX-overexpressing cells were treated as shown in panel **b** and caspase activity was measured. The error bars represent standard errors from four independent replicate experiments. **denotes $P<0.005$ comparing Nutlin to Nutlin + 17AAG in parental U2OS cells. (**d**) 17AAG inhibits AKT signaling. The indicated cell lines were treated with 2 $\mu$M of 17AAG for up to 24 h. Total AKT and p-AKT levels were assessed by immunoblots. PCNA is a loading control. (**e**) Inhibition of AKT phosphorylation potentiates Nutlin-induced apoptosis. RKO cells were treated with the PI3K inhibitor LY294002 for 1 h before adding 10 $\mu$M Nutlin for an additional 24 h. Left: Immunoblots. Right: Caspase activity. **denotes $P<0.005$ comparing Nutlin to Nutlin + PI3K inhibitor (LY)

entire treatment period, the drug combination was well tolerated. The reason for the observed tumor stabilization was that combined Nutlin + 17AAG treatment increased tumor cell death *in vivo* compared with Nutlin or 17AAG alone, which failed completely (Figure 6b).

In aggregate, our data showed that cooperative interactions between Nutlin and 17AAG effectively steer solid cancers away from a mere transient Nutlin-induced arrest program into therapeutically relevant apoptosis *in vivo*.

## Discussion

Small-molecule MDM2 inhibitors are an exciting new class of drugs to resurrect targeted p53 signaling in wtp53-retaining

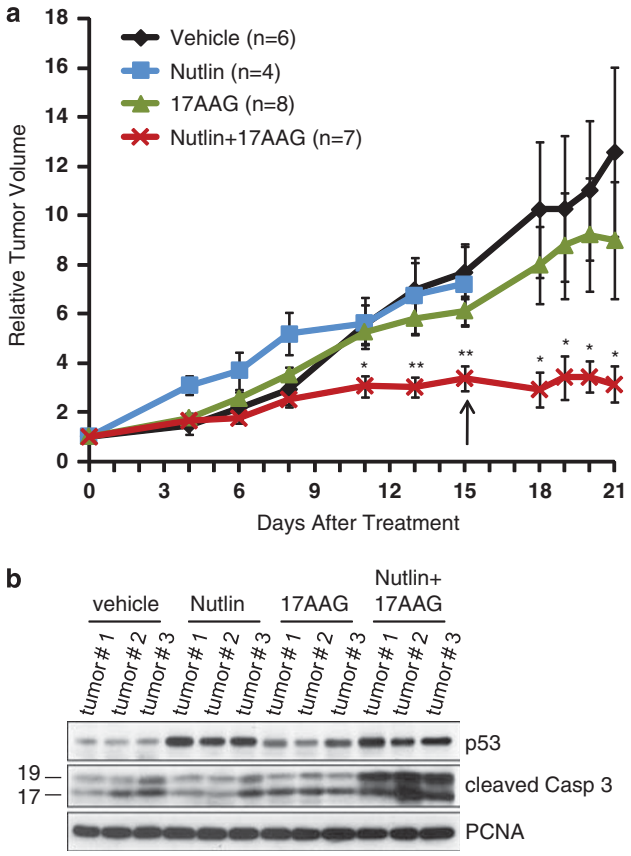


**Figure 6** Nutlin and 17AAG synergistically prevent tumor growth *in vivo* by inducing apoptosis. (**a**) Antitumor activity of Nutlin + 17AAG in human tumor xenografts. Nude mice were injected with $5 \times 10^6$ RKO cells per flank. Treatment started after 12 days when tumors were 200–300 $mm^3$ in volume (called day 0). The mice were randomized into four groups: vehicle, Nutlin alone, 17AAG alone and Nutlin + 17AAG. The graph indicates relative change in tumor volume compared with its corresponding initial tumor size prior to treatment. On day 15 (arrow), five mice needed to be killed because they had reached the tumor burden endpoint of 2 $cm^3$ (two Nutlin mice, one vehicle mouse and one 17AAG mouse). One Nutlin + 17AAG mouse needed to be killed owing to extensive necrosis despite unchanged tumor volume. The remaining mice were killed on day 21. Over the treatment period, mice receiving Nutlin + 17AAG showed no discernable changes in weight or behavior compared with the vehicle controls. The error bars indicate the standard error; $n=$ number of tumors analyzed. *denotes $P<0.05$; **denotes $P<0.005$. (**b**) Caspase activity is increased in tumors treated with Nutlin + 17AAG *versus* Nutlin or 17AAG alone. Protein was isolated from three randomized tumors per treatment. The highest level of caspase activity occurs in tumors treated with Nutlin + 17AAG compared with that in the vehicle control and in tumors treated with single drug. PCNA is a loading control

tumors. Nutlin, the most developed prototype, is a highly selective competitive inhibitor of the hydrophobic p53-binding pocket of MDM2. By inhibiting MDM2–p53 interaction, it shields p53 from MDM2 degradation, thereby non-genotoxically stabilizing and activating p53. Nutlin shows promise in hematological malignancies that rarely harbor p53 mutations and often show MDM2 overexpression.[5]

However, a fundamental problem of Nutlin is that the majority of non-hematopoietic wtp53 tumors merely mount a transient cytostatic response rather than the required cytotoxic antitumoral response.[9–11] A major known determinant mediating this cancer resistance *in vitro* and *in vivo* is MDMX, even in tumors without MDMX upregulation (Figure 5a).[15] MDMX is the MDM2 homolog that sequesters p53 and inhibits p53 transcription, but owing to the precise structural fit of Nutlin into the MDM2 pocket, is not efficiently inhibited by non-toxic doses. Additional factors that might protect solid tumors from undergoing Nutlin-induced apoptosis are oncogenic survival signaling pathways that counteract apoptotic p53 signaling. Thus, major efforts now focus on identifying and interfering with factors that contribute to apoptosis resistance during Nutlin treatment. This knowledge will contribute to developing Nutlin-based optimized combination therapies. Unfortunately, small-molecule and peptide inhibitors of MDMX are currently only in nascent developmental stages.[34–36] On the other hand, many studies already reported that selective inhibition of specific oncogenic survival pathways improves apoptotic resistance to Nutlin, mainly in hematologic tumor types. For example, inhibition of PI3K/AKT signaling enhanced apoptosis in ALL or CLL leukemia,[32,33] or inhibition of ERK signaling synergistically improves Nutlin-induced apoptosis in AML.[37]

We find here that 17AAG modulates p53 signaling during Nutlin treatment to overcome the apoptotic threshold, and identify 17AAG as a promising synthetic lethal partner of Nutlin. Our rationale for choosing 17AAG was based on the following: (i) Inhibition of Hsp90 was previously shown to cause wtp53 stabilization;[24,25] (ii) in a genetic mouse model, 17AAG was shown to kill transplanted primary medulloblastoma cells in a p53-dependent manner;[25] (iii) the Hsp90 chaperone complex is grossly overexpressed specifically in cancer cells; and (iv) most cancers depend on Hsp90 for survival, as numerous oncogenic client proteins, many of which negatively affect the p53 pathway, require permanent chaperone support. Among Hsp90 clients are many kinases that directly or indirectly phosphorylate and modulate the function of p53 and/or MDM2 and MDMX, for example, AKT/PKB, Chk1, GSK3b, ErbB2, mutant EGFR, p38MAPK and Raf/ERK.[18,31]

We show that in difficult-to-kill solid human cancer cells 17AAG modulates several components and pathways that favorably cooperate in Nutlin-activated p53 signaling to convert Nutlin's mere cytostatic response into a cytotoxic killing response. Although likely not a complete list, we could identify several factors that contribute to that: (i) In the context of Nutlin, 17AAG first and foremost destabilizes MDMX protein, but also reduces MDM2 protein levels; (ii) 17AAG induces proapoptotic p53 targets such as PUMA; (iii) 17AAG reduces p21 protein that at high levels might, at least in some cancers, favor a Nutlin-induced cell-cycle arrest; and (iv) 17AAG inhibits oncogenic survival pathways such as PI3K/AKT, which could normally counteract p53 signaling at multiple levels.

17AAG induces the robust enhancement of Nutlin-activated p53 transcription without changing p53 levels. Mechanistically, 17AAG interferes with the repressive Mdmx–p53 axis by disrupting MDMX–p53 complexes and inducing robust MDMX degradation.[26] Although RNAi-mediated knockdown was critical in demonstrating the central importance of MDMX in Nutlin resistance in experimental settings, it is currently not within clinical reach. Thus, to our knowledge the Nutlin + 17AAG combination represents the first effective pharmacological knockdown of MDMX.

The mechanism by which 17AAG induces MDMX degradation remains to be determined in the future. MDMX is not a known HSP90 client and therefore its 17AAG-mediated destabilization is likely indirect, for example by affecting posttranslational MDMX modifications. Concerning MDM2, it is a known Hsp90 client and Hsp90 inhibition by the 17AAG precursor geldanamycin stimulates MDM2 degradation.[20] Moreover, our co-immunoprecipitations show that 17AAG disrupts the MDM2–MDMX complex. This could contribute to MDM2 destabilization as one function of MDMX is to stabilize MDM2.[26] This could also explain rapid p53 stabilization, as MDM2–MDMX heterodimers are more a effective E3 ligase for p53 compared with MDM2 homodimers.[26] The latter could also explain why p53 is stabilized upon 17AAG treatment before MDMX degradation occurs in some of the cell lines. Although we were able to identify some important determinants, further elucidation of the synergistic mechanisms is warranted. 17AAG might also modulate p53 transcription through other mechanisms, for example, by affecting co-activators and/or p53 modifications.

The molecular rationale for this drug combination is quite compelling. 17AAG targets different tumor types by destabilizing multiple oncogenic pathways.[38] This suggests that the Nutlin + 17AAG combination might resurrect Nutlin as a clinically viable uniform platform against a broad spectrum of wtp53-harboring solid tumors. Moreover, 17AAG-type inhibitors specifically target tumor cells[31] for two reasons: Hsp90 upregulation is tumor-specific and 17AAG shows a 100-fold higher activity toward tumor cell-derived Hsp90 complexes than against Hsp90 purified from normal cells.[39] Thus, 17AAG may also help in better targeting of Nutlin responses specifically to tumor cells and reduce the bone marrow-based toxicity of Nutlin.

## Materials and Methods

**Cell culture and drugs.** The wtp53-harboring human cancer cell lines U2OS, RKO, HCT116 p53 + / + (and its isogenic match HCT116 p53 − / −), MCF7 and SJSA were maintained in DMEM, or RPMI-1640 for AGS and RPMI-1788, with 10% FBS at 37 °C in 5% $CO_2$. Stable U2OS cells expressing doxycycline-inducible MDMX were provided by Geoffrey Wahl and maintained in DMEM supplemented with 10% FBS. The following drugs were used: racemic Nutlin-3a (Sigma, St. Louis, MO, USA), 17-allylamino-17-demethoxygeldanamycin (LC Laboratories, Woburn, MA, USA), cycloheximide (Sigma), Z-VAD-FMK (R&D Systems, Minneapolis, MN, USA), ALLN (Calbiochem, San Diego, CA, USA) and LY294002 (Roche, Indianapolis, IN, USA). The human MDMX siRNA and scrambled siRNA were purchased from Qiagen (Valencia, CA, USA).

**Co-immunoprecipitations and immunoblots.** Cells were treated, lysed with 0.5% Triton X-100 in PBS supplemented with protease inhibitor cocktail (Roche) and sonicated. Whole-cell extracts (5–30 $\mu$g) were resolved on 10% SDS-PAGE gels and processed for ECL immunoblotting. For immunoprecipitation cells were lysed in the same buffer. Total protein (1 mg) was incubated overnight at 4°C with 1 $\mu$g of primary antibody and protein-A/G agarose beads (Roche). The beads were washed three times in buffer (0.5% Triton X-100 in PBS) and proteins were solubilized by boiling in 50 $\mu$l sample buffer prior to SDS-PAGE. The following antibodies were used: monoclonal p53 (DO1; Santa Cruz, Santa Cruz, CA, USA); monoclonal MDM2 (Ab-1; Calbiochem); rabbit Hdmx/Mdm4 (Bethyl Labs, Montgomery, TX, USA); rabbit cleaved PARP (D214; Cell Signaling, Danvers, MA, USA); monoclonal p21 (BD Biosciences, San Diego, CA, USA); rabbit Puma, Akt and phospho-AKT S473 (all Cell Signaling); and rabbit cleaved caspase-3 (Asp175; Cell Signaling). Monoclonal PCNA (PC10; Santa Cruz) was used as loading control. All antibodies were diluted 1 : 1000 to 1 : 5000.

**Real-time qRT-PCR.** Total RNA was isolated using Trizol and 10 $\mu$g was reverse-transcribed using random primers and SuperScript II Reverse Transcriptase (Invitrogen, Carlsbad, CA, USA). Real-time qRT-PCR was performed in triplicate using an MJ Research DNA Engine Opticon 2 using the Qiagen QuantiTect SyBr Green Mix. The cycling conditions were as follows: 94°C, 30 s; 55°C 30 s; 72°C 1 min and 68°C 10 s for 35 cycles. The human primer sequences used were as follows: MDMX – F: GCCTTGAGGAAGGATTGGTA, R: TCGACAATCAGGGACATCAT; PUMA, (BBC3) – F: ACGACCTCAACGCACAGT ACG, R: TCCCATGATGAGATTGTACAGGAC; P21(CDK1N1A) – F: CTGGAG ACTCTCAGGGTCGAAA, R: GATTAGGGCTTCCTCTTGGAGAA; and MDM2 – F: GGCGATTGGAGGGTAGACCT, R:CACATTTGCCTGGATCAGCA. The relative expression of all target genes was normalized to actin expression as internal efficiency control.

**Cell death assays.** Caspase assays were performed in triplicate using the fluorimetric Homogeneous Caspases Assay (Roche). Briefly, $4 \times 10^4$ cells plated per well in a 96-well plate were treated with 100 $\mu$l of media containing 2–10 $\mu$M 17AAG and/or Nutlin for 8–48 h. The substrate working solution was added and the plate was incubated at 37°C for 2–8 h or at room temperature overnight in the dark. The plates were read with a Spectramax M2 ROM using an excitation wavelength of 485 nm and emission wavelength of 520 nm. Annexin/PI assays were performed using FITC Annexin V (BD Biosciences) and PI (Sigma) following the protocol from BD Biosciences. After drug treatment, cells were trypsinized and diluted to $1 \times 10^6$ cells/ml in 1X binding buffer (0.01 M Hepes (pH 7.4), 0.14 M NaCl, 2.5 mM $CaCl_2$). Annexin (7.5 $\mu$l) and PI (10 $\mu$l of 50 $\mu$g/ml solution) were added to 150-$\mu$l cell suspension. After 15 min of incubation in the dark at room temperature, the cell suspensions were adjusted to 500 $\mu$l with 1X binding buffer and counted using a FacScan analyzer (argon laser; Becton Dickinson, Franklin Lane, NJ, USA).

To evaluate the combinatorial synergy between the two drugs, the percentage of dead cells was determined by trypan blue exclusion assay. $IC_{50}$ values were determined and isobologram and combination index (CI) analyses were performed using the CalcuSyn software as described by Chou.[27]

**Xenograft assays.** Six- to seven-week-old athymic male nude mice (nu/nu) were purchased from Harlan Laboratories (Indianapolis, IN, USA). All animal experiments were approved by the Stony Brook University Internal Review Board. RKO cells ($5 \times 10^6$ per flank) suspended in 50% Matrigel (BD Biosciences) were injected subcutaneously into the four flanks of mice. Tumors were measured by a caliper and volume (V) was calculated using the formula V = length (L) × width $(W)^2/2$, where width was the smaller dimension of the tumor. When tumors had reached a volume between 200 and 300 $mm^3$, treatment was started. The change in tumor volume was calculated by comparing the tumor size during treatment with the original tumor size before treatment began ( = day 0). The tumors were measured 3–4 times per week. Mice were randomized into four treatment groups: vehicle, Nutlin, 17AAG and Nutlin + 17AAG. Student's two-tailed *t*-test with equal variance was used to determine the statistical significance of the relative tumor size changes between the vehicle-treated *versus* drug-treated tumors.

Racemic Nutlin-3 (Cayman Chemical, Ann Arbor, MI, USA; cat. no. 10004372) was injected at 35 mg/kg per mouse in 10% DMSO. 17AAG (NSC 330507) and the egg phospholipid diluent (EPL) vehicle (NSC 704057) were supplied by the Pharmaceutical Management Branch, Cancer Therapy Evaluation Program of The National Cancer Institute. 17AAG was injected at 80 mg/kg in 10% DMSO plus 90% EPL. The mice in the vehicle group were injected with vehicles for both Nutlin and 17AAG.

On days 0–10 treatment was performed by intraperitoneal injection (IP). Nutlin was injected by IP every other day. 17AAG was injected on days 0–2 and 4–8. IP injection of vehicle followed the same schedule as Nutlin and 17AAG. On days 11–18, doses were split between IP and IT (intratumoral injection). Nutlin, 17AAG or vehicle were injected on days 12–13, 15 and 17–18. The mice were killed on day 21. Tumors were isolated and sonicated in 0.5% Triton X-100/PBS using the protease inhibitor cocktail (Roche) and analyzed by immunoblotting.

## Conflict of Interest

The authors declare no conflict of interest.

**Acknowledgements**. This work was funded by grants from the National Cancer Institute (CA0664 and CA93853 to UMM), Deutsche Krebshilfe (108173 to

UMM), Deutsche Forschungsgemeinschaft (MO 1998/1 to UMM) and the Carol Baldwin Breast Cancer Research Fund (to NDM). ARY is a recipient of an NCI T32 Post-doctoral Fellowship. The 17-AAG and EPL solution were provided by Bristol-Myers Squibb and the National Cancer Institute, NIH.

1. Goldstein I, Marcel V, Olivier M, Oren M, Rotter V, Hainaut P. Understanding wild-type and mutant p53 activities in human cancer: new landmarks on the way to targeted therapies. *Cancer Gene Ther* 2011; **18**: 2–11.
2. Martins CP, Brown-Swigart L, Evan GI. Modeling the therapeutic efficacy of p53 restoration in tumors. *Cell* 2006; **127**: 1323–1334.
3. Ventura A, Kirsch DG, McLaughlin ME, Tuveson DA, Grimm J, Lintault L *et al.* Restoration of p53 function leads to tumour regression *in vivo*. *Nature* 2007; **445**: 661–665.
4. Carvajal D, Tovar C, Yang H, Vu BT, Heimbrook DC, Vassilev LT. Activation of p53 by MDM2 antagonists can protect proliferating cells from mitotic inhibitors. *Cancer Res* 2005; **65**: 1918–1924.
5. Vassilev LT. Small-molecule antagonists of p53–MDM2 binding: research tools and potential therapeutics. *Cell Cycle* 2004; **3**: 419–421.
6. Vassilev LT, Vu BT, Graves B, Carvajal D, Podlaski F, Filipovic Z *et al. In vivo* activation of the p53 pathway by small-molecule antagonists of MDM2. *Science* 2004; **303**: 844–848.
7. Saha MN, Micallef J, Qiu L, Chang H. Pharmacological activation of the p53 pathway in haematological malignancies. *J Clin Pathol* 2010; **63**: 204–209.
8. Vassilev LT. MDM2 inhibitors for cancer therapy. *Trends Mol Med* 2007; **13**: 23–31.
9. Tovar C, Rosinski J, Filipovic Z, Higgins B, Kolinsky K, Hilton H *et al.* Small-molecule MDM2 antagonists reveal aberrant p53 signaling in cancer: implications for therapy. *Proc Natl Acad Sci USA* 2006; **103**: 1888–1893.
10. Huang B, Deo D, Xia M, Vassilev LT. Pharmacologic p53 activation blocks cell cycle progression but fails to induce senescence in epithelial cancer cells. *Mol Cancer Res* 2009; **7**: 1497–1509.
11. Demidenko ZN, Korotchkina LG, Gudkov AV, Blagosklonny MV. Paradoxical suppression of cellular senescence by p53. *Proc Natl Acad Sci USA* 2010; **107**: 9660–9664.
12. Xia M, Knezevic D, Vassilev LT. p21 does not protect cancer cells from apoptosis induced by nongenotoxic p53 activation. *Oncogene* 2011; **30**: 346–355.
13. Wade M, Wong ET, Tang M, Stommel JM, Wahl GM. Hdmx modulates the outcome of p53 activation in human tumor cells. *J Biol Chem* 2006; **281**: 33036–33044.
14. Hu B, Gilkes DM, Farooqi B, Sebti SM, Chen J. MDMX overexpression prevents p53 activation by the MDM2 inhibitor Nutlin. *J Biol Chem* 2006; **281**: 33030–33035.
15. Patton JT, Mayo LD, Singhi AD, Gudkov AV, Stark GR, Jackson MW. Levels of HdmX expression dictate the sensitivity of normal and transformed cells to Nutlin-3. *Cancer Res* 2006; **66**: 3169–3176.
16. Laurie NA, Shih CS, Dyer MA. Targeting MDM2 and MDMX in retinoblastoma. *Curr Cancer Drug Targets* 2007; **7**: 689–695.
17. Hu B, Gilkes DM, Chen J. Efficient p53 activation and apoptosis by simultaneous disruption of binding to MDM2 and MDMX. *Cancer Res* 2007; **67**: 8810–8817.
18. Whitesell L, Lindquist SL. HSP90 and the chaperoning of cancer. *Nat Rev Cancer* 2005; **5**: 761–772.
19. Blagosklonny MV, Toretsky J, Bohen S, Neckers L. Mutant conformation of p53 translated *in vitro* or *in vivo* requires functional HSP90. *Proc Natl Acad Sci USA* 1996; **93**: 8379–8383.
20. Peng Y, Chen L, Li C, Lu W, Chen J. Inhibition of MDM2 by hsp90 contributes to mutant p53 stabilization. *J Biol Chem* 2001; **276**: 40583–40590.
21. Walerych D, Kudla G, Gutkowska M, Wawrzynow B, Muller L, King FW *et al.* Hsp90 chaperones wild-type p53 tumor suppressor protein. *J Biol Chem* 2004; **279**: 48836–48845.
22. Muller L, Schaupp A, Walerych D, Wegele H, Buchner J. Hsp90 regulates the activity of wild type p53 under physiological and elevated temperatures. *J Biol Chem* 2004; **279**: 48846–48854.
23. Sasaki M, Nie L, Maki CG. MDM2 binding induces a conformational change in p53 that is opposed by heat-shock protein 90 and precedes p53 proteasomal degradation. *J Biol Chem* 2007; **282**: 14626–14634.
24. Lin K, Rockliffe N, Johnson GG, Sherrington PD, Pettitt AR. Hsp90 inhibition has opposing effects on wild-type and mutant p53 and induces p21 expression and cytotoxicity irrespective of p53/ATM status in chronic lymphocytic leukaemia cells. *Oncogene* 2008; **27**: 2445–2455.
25. Ayrault O, Godeny MD, Dillon C, Zindy F, Fitzgerald P, Roussel MF *et al.* Inhibition of Hsp90 via 17-DMAG induces apoptosis in a p53-dependent manner to prevent medulloblastoma. *Proc Natl Acad Sci USA* 2009; **106**: 17037–17042.
26. Wade M, Wang YV, Wahl GM. The p53 orchestra: Mdm2 and Mdmx set the tone. *Trends Cell Biol* 2010; **20**: 299–309.
27. Chou TC. Drug combination studies and their synergy quantification using the Chou–Talalay method. *Cancer Res* 2010; **70**: 440–446.
28. Chen X, Ko LJ, Jayaraman L, Prives C. p53 levels, functional domains, and DNA damage determine the extent of the apoptotic response of tumor cells. *Genes Dev* 1996; **10**: 2438–2451.
29. Vaseva AV, Marchenko ND, Moll UM. The transcription-independent mitochondrial p53 program is a major contributor to nutlin-induced apoptosis in tumor cells. *Cell Cycle* 2009; **8**: 1711–1719.
30. Laurie NA, Donovan SL, Shih CS, Zhang J, Mills N, Fuller C *et al.* Inactivation of the p53 pathway in retinoblastoma. *Nature* 2006; **444**: 61–66.
31. Kamal A, Burrows FJ. Hsp90 inhibitors as selective anticancer drugs. *Discov Med* 2004; **4**: 277–280.
32. Zhu N, Gu L, Li F, Zhou M. Inhibition of the Akt/survivin pathway synergizes the antileukemia effect of nutlin-3 in acute lymphoblastic leukemia cells. *Mol Cancer Ther* 2008; **7**: 1101–1109.
33. Zauli G, Voltan R, Bosco R, Melloni E, Marmiroli S, Rigolin GM *et al.* Dasatinib plus Nutlin-3 shows synergistic anti-leukemic activity in both p53wild-type and p53mutated B chronic lymphocytic leukemias by inhibiting the Akt pathway. *Clin Cancer Res* 2010; **70**: 440–446.
34. Popowicz GM, Czarna A, Wolf S, Wang K, Wang W, Domling A *et al.* Structures of low molecular weight inhibitors bound to MDMX and MDM2 reveal new approaches for p53–MDMX/MDM2 antagonist drug discovery. *Cell Cycle* 2010; **9**: 1104–1111.
35. Reed D, Shen Y, Shelat AA, Arnold LA, Ferreira AM, Zhu F *et al.* Identification and characterization of the first small molecule inhibitor of MDMX. *J Biol Chem* 2010; **285**: 10786–10796.
36. Wang H, Ma X, Ren S, Buolamwini JK, Yan C. A small-molecule inhibitor of MDMX activates p53 and induces apoptosis. *Mol Cancer Ther* 2011; **10**: 69–79.
37. Zhang W, Konopleva M, Burks JK, Dywer KC, Schober WD, Yang JY *et al.* Blockade of mitogen-activated protein kinase/extracellular signal-regulated kinase kinase and murine double minute synergistically induces apoptosis in acute myeloid leukemia via BH3-only proteins Puma and Bim. *Cancer Res* 2010; **70**: 2424–2434.
38. Isaacs JS, Xu W, Neckers L. Heat shock protein 90 as a molecular target for cancer therapeutics. *Cancer Cell* 2003; **3**: 213–217.
39. Kamal A, Thao L, Sensintaffar J, Zhang L, Boehm MF, Fritz LC *et al.* A high-affinity conformation of Hsp90 confers tumour selectivity on Hsp90 inhibitors. *Nature* 2003; **425**: 407–410.



Supplementary Information accompanies the paper on Cell Death and Disease website (http://www.nature.com/cddis)